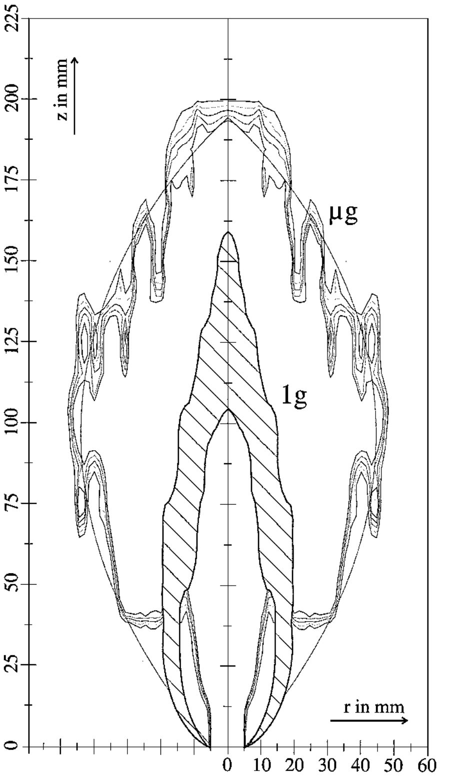

Fig. 2 Stoichiometric minimum and maximum flame contours under gravity and flame contour under microgravity.

combustion chamber. These contours are only a small region in the concentration profile, and the measured data include much more information, such as the burnout and the thickness of the flames. As expected, the calculated thermal and stoichiometric contours differ from the visual ones. These have to be considered for the verification of the numerical models by experimentally determined contours.

Summary

The investigated hydrogen air flames are strongly influenced by buoyancy. Gravity flames show a characteristic flickering, which disappears under microgravity. This fact confirms the correlation with the buoyancy. It may be concluded from visual investigations that the flames under microgravity are bigger and less bright than flames under gravity. The microthermocouples employed are well suited for the measurement of the two-dimensional temperature profile inside the combustion chamber. This method is relatively inexpensive in comparison to the different laser techniques inasmuch as the application of lasers under microgravity is just beginning. Nevertheless, the measured temperature profile describes the evolution of the flame contour quantitatively. The oxygen concentration profile of a hydrogen diffusion flame was determined by means of solid electrolyte sensors and, hence, the contour of the flame. The sensor signals show the quantitative differences between the gravity and microgravity cases. The data show that there is flickering under gravity and continuous growth under microgravity. In the gravity case, it is possible to calculate a minimum and a maximum contour. The microgravity contour at the end of the drop is larger than that under normal gravity conditions. This shows that gaspotentiometry with solid electrolyte sensors is very useful, especially because the sensors are easier to handle and more cost effective than laser-based methods. This method has great potential; however, it is not a nonintrusive method, and the influences on the investigated processes should be evaluated. The described techniques allow a quantitative analysis of the flame behavior under gravity and microgravity and add information about the flame to the usual video techniques. The collected data can be used for evaluation of numerical simulations and flame length calculations. The data show significant differences between visual observations and thermal and stoichiometrical contours. This must be taken into account for the comparison with numerical simulations.

Acknowledgments

This project is supported under Contract 50WM9447 by the Deutsches Zentrum fuer Luft und Raumfahrt DLR. In addition we wish to thank the drop tower team at the Center of Applied Space Technology and Microgravity in Bremen for their cooperation.

References

[1]Burke, S. P., and Schumann, T. E. W., "Diffusion Flames," *Industrial and Engineering Chemistry*, Vol. 20, No. 10, 1928, pp. 998–1004.

[2]Stocker, D. P., "The Effect of Reduced Gravity on the Shape of Laminar Burke–Schumann Diffusion Flames," *Spring Technical Meeting of the Central States Section of the Combustion Institute*, Combustion Inst., Pittsburgh, PA, 1991, pp. 99–104.

[3]Bahadori, M. Y., Edelman, R. B., Stocker, D. P., and Olson, S. L., "Ignition and Behavior of Laminar Gas-Jet Diffusion Flames in Microgravity," *AIAA Journal*, Vol. 28, No. 2, 1989, pp. 236–244.

[4]Rau, H., "Untersuchungen zur Verbrennung in Flammen unter Anwendung der Gaspotentiometrie," Dissertation B, Otto-von-Guericke-Univ. Magdeburg, Magdeburg, Germany, 1984.

[5]Lorenz, H., Tittmann, K., Sitzki, L., Trippler, S., and Rau, H., "Gaspotentiometric Method with Solid Electrolyte Oxygen Sensors for Investigation of Combustion," *Fresenius Journal of Analytical Chemistry*, Vol. 356, Nos. 3, 4, 1996, pp. 215–220.

[6]Hess, K., "Flammenlänge und Flammenstabilität," Dissertation, Technische Hochschule Karlsruhe, Karlsruhe, Germany, 1964.

[7]Katta, V. R., and Roquemore, W. M., "Role of Inner and Outer Structures in Transitional Jet Diffusion Flame," *Combustion and Flame*, Vol. 92, 1993, pp. 274–282.

[8]Buckmaster, J., and Peters, N., "The Infinite Candle and Its Stability—A Paradigm for Flickering Diffusion Flames," *21th Symposium on Combustion*, Combustion Inst., Pittsburgh, PA, 1986, pp. 1829–1836.

K. Kailasanath
Associate Editor

Explicit Equation for Flow Through American Society of Mechanical Engineers Nozzle Meters

W. Bussman* and J. White†
Koch–Glitsch, Inc., Wichita, Kansas 67220

Nomenclature

A_D	= area of pipe containing American Society of Mechanical Engineers (ASME) nozzle meter, m^2
A_d	= area of ASME nozzle meter throat, m^2
C	= ASME nozzle meter discharge coefficient
D	= diameter of pipe containing ASME nozzle meter, m
d	= throat diameter of ASME nozzle meter, m
q_m	= mass flow rate of fluid in pipe, kg/s
Re_1	= Reynolds number based on pipe diameter, $V_1 D/\upsilon_1$
V_1	= actual upstream fluid velocity in pipe, m/s
Δp	= differential pressure, Pa
β	= d/D
ε_1	= expansion factor based on upstream pressure
ρ_1	= density of flowing fluid upstream of ASME nozzle meter, kg/m^3

Received Feb. 9, 1998; revision received May 15, 1998; accepted for publication May 18, 1998.

*Research and Development Engineer, John Zink Company Division, 11920 East Apache, P.O. Box 21220, Tulsa, OK 74121-1220.

†Senior Design Engineer, John Zink Company Division, 11920 East Apache, P.O. Box 21220, Tulsa, OK 74121-1220.

Introduction

THE mass flow rate of a fluid in a pipe using a nozzle meter is determined by the following equation[1] in SI units:

$$q_m = \frac{\pi}{4} C \varepsilon_1 d^2 \sqrt{\frac{2\Delta p \rho_1}{1-\beta^4}} \tag{1}$$

Within the limits of the American Society of Mechanical Engineers (ASME) standards, the discharge coefficient C is dependent on the upstream Reynolds number Re_1 in the pipe, which is itself dependent on the mass flow rate. Therefore, when determining the mass flow rate, the solution is usually obtained by iteration from an initial chosen value of discharge coefficient or Reynolds number. Most data acquisition systems allow a limited amount of data conditioning and recording of calculated values. However, the limited data conditioning is only rarely capable of effective iteration, especially at high sampling rates. This Note describes the development of an exact analytical equation that can be used for determining the flow rate of a fluid through a pipe using a nozzle meter without the need for iterations.

Derivation of Mathematical Solution

The following analysis is conducted using the SI form of the equation. The U.S.-units-of-measure form of the equation is analogous. When used in accordance with the ASME standard, the coefficient of discharge of ASME flow nozzles with wall taps is given by the following:

$$C = 0.9975 - 0.00653\left(10^6\beta \big/ Re_1\right)^{0.5} \tag{2}$$

Equation (2) is valid for β values between 0.2 and 0.8 and Reynolds numbers between 10^4 and 6×10^6. These β and Reynolds number values correspond to a maximum and minimum discharge coefficient of 0.9963 and 0.9391, respectively. Theory suggests that the exponent should go to 0.2 for Reynolds numbers greater than 10^6, but the difference is so small that it is difficult to confirm experimentally.

Substituting Eq. (2) into Eq. (1) and rearranging gives

$$q_m = k_1 C = k_1 k_2 - \left(k_1 k_3 \big/ \sqrt{Re_1}\right) \tag{3}$$

where $k_1 = A_d \varepsilon_1 \sqrt{[2\Delta p \rho_1/(1-\beta^4)]}$, $k_2 = 0.9975$, and $k_3 = 0.00653\sqrt{(10^6\beta)}$. Substituting the definition for Reynolds number ($Re_1 = V_1 D/\upsilon_1$) and mass flow rate ($q_m = \rho_1 V_1 A_D$) into Eq. (3) and rearranging gives a cubic equation in $\sqrt{V_1}$. Letting $x = \sqrt{V_1} > 0$, we can write

$$x^3 + ax + b = 0 \tag{4}$$

where $a = (-k_1 k_2)/\rho_1 A_D$ and $b = [k_1 k_3 \sqrt{(\upsilon_1/D)}]/\rho_1 A_D$.

It can be shown that the cubic discriminant is less than zero for all nozzle meters that comply with the ASME standards. The discriminant D' for the cubic equation is

$$D' = (b^2/4) + (a^3/27) < 0 \tag{5}$$

Substituting the equations for a, b, k_1, k_2, and k_3 and Eq. (3) into Eq. (5) and simplifying gives

$$290\beta C < Re_1 \tag{6}$$

Thus, the discriminant has a negative value whenever the Reynolds number Re_1 is larger than 290. However, the equation for C, given by ASME standards, requires that the Reynolds number Re_1 be greater than 10^4. Therefore, one can conclude that the discriminant is always negative. For this condition there will be three real and unequal roots. The three real roots will have the following values[2]:

$$x = 2\sqrt{(-a/3)}\cos[(\phi/3) + N] \tag{7}$$

where

$$\cos(\phi) = \frac{-b}{2\sqrt{-a^3/27}} \tag{8}$$

and N is 0, 120, or 240 deg.

Process of Elimination of Roots

Substituting the equations for a, b, k_2, and k_3 and Eq. (3) into Eq. (8) and simplifying gives

$$\cos(\phi) = -17.029\sqrt{\beta C/Re_1} \tag{9}$$

Each of the factors, β, C, and Reynolds number Re_1, has a limited range, and β must lie between 0.2 and 0.8. The Reynolds number Re_1 must lie between 1×10^4 and 6×10^6. For this range of Reynolds number Re_1, coefficient C must lie between 0.9391 and 0.9963 as stated earlier. Using Eq. (9) and extreme values for β, C, and Reynolds number Re_1, one can demonstrate that $\cos(\phi)$ must lie between -0.15203 and -0.003013. For example, the lower limit is calculated using the maximum values for β and C and the minimum value for Reynolds number Re_1. Thus, the lower limit for $\cos(\phi)$ is $-17.029\sqrt{(0.8 \times 0.9963/1 \times 10^4)} = -0.15203$. With this limited range for $\cos(\phi)$, the principal value for ϕ lies in the range of 90.17–98.74 deg.

If we let

$$t = \cos(\phi/3 + N) \tag{10}$$

substitute term a into Eq. (7), and simplify, we can write the following equation:

$$x = 2t\sqrt{\frac{V_1(0.9975)}{3C}} \tag{11}$$

If we substitute $x = \sqrt{V_1}$ into Eq. (11) and solve for term t, we get

$$t = (0.86711)\sqrt{C} \tag{12}$$

As mentioned earlier, the maximum and minimum values of C are 0.9963 and 0.9391, respectively. These values of C correspond to a maximum and minimum value of t equal to 0.8655 and 0.8403, respectively. We will use this range of t to eliminate two of the possible roots.

For $N = 120$ deg, term t from Eq. (10) is in the range from -0.8903 to -0.8665. Thus, no solution for $N = 120$ deg is valid. For $N = 240$ deg, term t from Eq. (10) is in the range from 0.0010 to 0.0508. Thus, no solution for $N = 240$ deg is valid. Finally, for $N = 0$ deg, term t from Eq. (10) is in the range from 0.8395 to 0.8655. Therefore, we can conclude that N must be equal to 0 deg.

Final Form of Equations

The terms involved in the solution for V_1 may be simplified as follows:

$$a = -0.9975\varepsilon_1\sqrt{\frac{2\Delta p\beta^4}{\rho_1(1-\beta^4)}} \tag{13}$$

$$b = -6.546a\sqrt{\beta\upsilon_1/D} \tag{14}$$

$$\phi = \arccos\left(\frac{-b}{2\sqrt{-a^3/27}}\right) \tag{15}$$

where $\phi \in [90, 180]$ (deg), and finally,

$$V_1 = x^2 = \frac{-4a\cos^2(\phi/3)}{3} \tag{16}$$

Once V_1 is determined, mass flow rate can be calculated directly from the continuity equation.

Conclusions

An exact analytical solution for flow through an ASME standard nozzle meter exists. The traditional use of iterative methods or approximations of C as constant is no longer required. This solution is helpful for installations that use ASME nozzle meter readings to record flow data. Using the explicit equation presented here, direct flow readouts can be provided that account for variations of all measured parameters.

References

[1]"Measurement of Fluid Flow in Pipes Using Orifice, Nozzle, and Venturi," American Society of Mechanical Engineers, ASME MFC-3M-1989, New York, 1990, pp. 32–36.

[2]Hodgman, C. D., *Mathematical Tables*, Chemical Rubber Publishing, Cleveland, OH, 1948, p. 277.

J. P. Gore
Associate Editor

Accounting for Effects of a System Rotation on the Pressure-Strain Correlation

B. A. Younis*
City University,
London EC1V 0HB, England, United Kingdom
C. G. Speziale†
Boston University, Boston, Massachusetts 02215
and
S. A. Berger‡
University of California, Berkeley,
Berkeley, California 94720

Introduction

TURBULENT shear layers are known to be very sensitive to the imposition of a system rotation. The classic experiments of Johnston et al.,[1] for example, conducted in a channel rotated about a spanwise axis, show that the turbulence is augmented on the pressure side and diminished on the suction side, relative to the nonrotating flow. At high rates of rotation, turbulence is extinguished altogether on the suction side, and the flow is seen to assume a laminar-like state. Effects such as these have highlighted serious shortcomings in eddy-viscosity-based closures as these, in most cases, contain no explicit dependence on rotation.[2] Such a dependence is present in the exact equations for the Reynolds stresses, and thus closures based on the solution of either the algebraic[3] or the differential[4] forms of these equations can be relied on to reproduce, qualitatively at any rate, the correct response to a system rotation. In this Note, we consider certain aspects of modeling the effects of a system rotation on the Reynolds-stress equations and put forward proposals for extending the applicability of existing pressure-strain models to rotating coordinate systems. We check the proposals by computing a fully developed $\{U_i = [U(y),\ 0,\ 0]\}$ turbulent flow inside a long, straight channel subjected to rotation about a spanwise axis, i.e., $\Omega_i = (0,\ 0,\ \Omega)$. The channel has an infinite aspect ratio, and so no secondary flows are generated. Comparisons are made with the experimental data of Johnston et al.[1] and with the recent direct numerical simulations of Kristoffersen and Andersson.[5] Interest in this flow stems from its being numerically trivial to represent yet one that is representative of many practically relevant flows whose behavior is strongly dominated by a system rotation.[6,7] This study extends the validation to higher rotation rates than hitherto reported in the literature and, in doing so, obtains a somewhat unexpected result.

Received Jan. 5, 1998; revision received May 10, 1998; accepted for publication May 14, 1998.

*Senior Lecturer, Department of Civil Engineering.

†Professor, Aerospace and Mechanical Engineering Department. Member AIAA.

‡Professor, Department of Mechanical Engineering. Fellow AIAA.

Present Proposal

The equation for the Reynolds stresses in a rotating frame of reference are

$$\overbrace{U_k \frac{\partial \overline{u_i u_j}}{\partial x_k}}^{\text{Convection: } C_{ij}} = -\overbrace{\left(\overline{u_i u_k}\frac{\partial U_j}{\partial x_k} + \overline{u_j u_k}\frac{\partial U_i}{\partial x_k}\right)}^{\text{Shear production: } P_{ij}}$$
$$-\overbrace{2\Omega_k\left(\overline{u_j u_m}\epsilon_{ikm} + \overline{u_i u_m}\epsilon_{jkm}\right)}^{\text{Rotation production: } G_{ij}}$$
$$-\overbrace{\frac{\partial}{\partial x_k}\left[\overline{u_i u_j u_k} + \frac{1}{\rho}\left(\overline{p' u_i}\delta_{jk} + \overline{p' u_j}\delta_{ik}\right) - \nu\frac{\partial \overline{u_i u_j}}{\partial x_k}\right]}^{\text{Diffusion: } D_{ij}}$$
$$-\underbrace{2\nu\left(\overline{\frac{\partial u_i}{\partial x_k}\frac{\partial u_j}{\partial x_k}}\right)}_{\text{Dissipation: } \epsilon_{ij}} + \underbrace{\overline{\frac{p'}{\rho}\left(\frac{\partial u_i}{\partial x_j} + \frac{\partial u_j}{\partial x_i}\right)}}_{\text{Redistribution: } \Phi_{ij}} \tag{1}$$

We focus here on modeling the fluctuating pressure-strain correlations term Φ_{ij} in the preceding equation. The explicit appearance of the fluctuating pressure can be eliminated by taking the divergence for the fluctuating velocity u_i, thus obtaining a Poisson equation for p'. With the assumption of homogeneous turbulence, the solution to this equation can be expressed as

$$\Phi_{ij} \equiv \overline{\frac{p'}{\rho}\left[\frac{\partial u_i}{\partial x_j} + \frac{\partial u_j}{\partial x_i}\right]} = -\frac{1}{4\pi}\int \overline{\frac{\partial^2 (u_k u_l)'}{\partial x_k' x_l'}\left[\frac{\partial u_i}{\partial x_j} + \frac{\partial u_j}{\partial x_i}\right]}\frac{\mathrm{dvol}}{\boldsymbol{r}}$$
$$-\frac{1}{2\pi}\int \frac{\partial U_k'}{\partial x_l'}\overline{\frac{\partial u_l'}{\partial x_k'}\left[\frac{\partial u_i}{\partial x_j} + \frac{\partial u_j}{\partial x_i}\right]}\frac{\mathrm{dvol}}{\boldsymbol{r}}$$
$$-\frac{1}{2\pi}\epsilon_{ijk}\Omega_j\int \overline{\frac{\partial u_k'}{\partial x_l'}\left[\frac{\partial u_i}{\partial x_j} + \frac{\partial u_j}{\partial x_i}\right]}\frac{\mathrm{dvol}}{\boldsymbol{r}} \tag{2}$$

It is immediately clear that the effects of rotation must be accounted for explicitly in the models for Φ_{ij}. These models are fairly well established for stationary flows, and the question that arises here is how best to extend these to flows with a system rotation. In addressing this question, note that, in a rotating frame, both P_{ij} and G_{ij} (quantities that commonly appear in the models for Φ_{ij}) are dependent on the frame's rotation rate, whereas turbulence is, of course, entirely independent of the choice of coordinates system used to analyze the flow. A primary requirement in the model, therefore, is that it should yield identical results irrespective of whether it is used in conjunction with a fixed or rotating frame of reference. In this connection, it is helpful to discard the traditional, term-by-term approach to modeling Φ_{ij} in favor of a more widely based formulation that recognizes that a complete model for Φ_{ij} may be obtained as a combination of terms involving the turbulence anisotropy b_{ij}, the mean rate of strain tensor S_{ij}, and the mean vorticity tensor W_{ij}, viz.,

$$\Phi_{ij} = -\left(C_1\epsilon + C_1^* P_k\right)b_{ij} + C_2\epsilon\left(b_{ik}b_{kj} - \tfrac{1}{3}b_{kl}b_{kl}\delta_{ij}\right)$$
$$+\left(C_3 - C_3^* II_b^{\frac{1}{2}}\right)kS_{ij} + C_4 k\left(b_{ik}S_{jk} + b_{jk}S_{ik} - \tfrac{2}{3}b_{kl}S_{kl}\delta_{ij}\right)$$
$$+ C_5 k\left(b_{ik}W_{jk} + b_{jk}W_{ik}\right) \tag{3}$$

where

$$S_{ij} = \frac{1}{2}\left(\frac{\partial U_i}{\partial x_j} + \frac{\partial U_j}{\partial x_i}\right), \qquad W_{ij} = \frac{1}{2}\left(\frac{\partial U_i}{\partial x_j} - \frac{\partial U_j}{\partial x_i}\right)$$
$$b_{ij} = \frac{\overline{u_i u_j}}{\overline{u_q u_q}} - \frac{1}{3}\delta_{ij}, \qquad II_b = b_{ij}b_{ij} \tag{4}$$

Thus the linear model of Launder et al.[8] (hereafter LRR), its simplification (LRR-IP), and the quadratic model of Speziale et al.[9]